The Matsuno-Gill model and equatorial superrotation

Adam P. Showman[1,2] and Lorenzo M. Polvani[2,3]

Received 14 June 2010; revised 26 July 2010; accepted 3 August 2010; published 25 September 2010.

[1] Equatorial superrotation can be generated in global general circulation models (GCMs) when forced with longitudinally varying heating, similar to that postulated in the Matsuno-Gill model. However, the implications of the classical Matsuno-Gill theory for equatorial superrotation have not, to date, been addressed. Here, we show that the classic, shallow-water Matsuno-Gill solutions do not exhibit equatorial superrotation: although the flow converges westerly momentum from high latitudes to the equator—promoting superrotation—they also contain an artificial source of easterly momentum at the equator that cancels the latitudinal momentum convergence and prevents superrotation from emerging. This artificial momentum source results from a physically inconsistent representation of vertical momentum transport in the model. We show that if the Matsuno-Gill model is modified to properly account for momentum exchange with an underlying quiescent layer, the solutions naturally exhibit equatorial superrotation, at any forcing amplitude. **Citation:** Showman, A. P., and L. M. Polvani (2010), The Matsuno-Gill model and equatorial superrotation, *Geophys. Res. Lett.*, *37*, L18811, doi:10.1029/2010GL044343.

1. Introduction

[2] Idealized models of the tropospheric response to zonally varying tropical heating provide significant insight into the Walker and monsoonal circulations, tropical-extratropical teleconnections, and other aspects of tropical dynamics. The simplest and best-known of these are one-layer shallow-water models damped by radiative relaxation and linear (Rayleigh) friction. Analytic solutions were pioneered by *Matsuno* [1966] and *Gill* [1980] and have become a canonical problem in tropical dynamics. When the imposed heating is symmetric about the equator, the response can be interpreted as steady, damped Kelvin and Rossby waves extending to the east and west, respectively, of the region of heating.

[3] When zonally varying, steady heat sources of the type postulated in the Matsuno-Gill model are used in idealized general circulation models (GCMs), equatorial superrotation—westerly flow at the equator corresponding to a local maximum of angular momentum per unit mass—emerges in the upper troposphere [*Suarez and Duffy*, 1992; *Saravanan*, 1993; *Kraucunas and Hartmann*, 2005; *Norton*, 2006; *Biello et al.*, 2007]. Maintaining such a jet against frictional processes requires up-gradient momentum transport by waves or eddies. *Held* [1999] suggested that the equatorial superrotation in these simplified GCMs results from poleward radiation of Rossby waves forced by the imposed tropical heating, and their dissipation or breaking at higher latitudes. Although tropical wave forcing is not dominant in the current climate [*Lee*, 1999], superrotation could emerge if the tropical wave forcing were greater, as possibly relevant to past or future climates [*Tziperman and Farrell*, 2009; *Caballero and Huber*, 2010].

[4] Despite the direct connection between the idealized Matsuno-Gill models and these GCM results—both in the zonally varying tropical heating and in the existence of a Rossby-wave response—it appears that the implications of the classic Matsuno-Gill model for meridional fluxes of momentum have not previously been examined in the literature. Our modest aim is to fill the gap between the canonical Matsuno-Gill models and the GCM results by clarifying the implications of the Matsuno-Gill solutions for equatorial superrotation. First, we show that equatorial superrotation does not occur in the traditional one-layer shallow-water model with Matsuno-Gill-type forcing. We diagnose the reasons why and show that the lack of superrotation results from an artificial easterly torque associated with an inconsistent representation of vertical momentum transport. Second, we demonstrate that when the original Matsuno-Gill equations are modified to properly capture momentum exchange with an underlying quiescent layer, superrotation emerges. This is the first demonstration of superrotation in response to Matsuno-Gill-type forcing in a one-layer system, and the simplicity of our model yields new insights into the mechanisms that enable the existence of superrotating flows.

2. Model and Methods

[5] We adopt a 1-1/2 layer shallow-water model, consisting of an active layer representing the upper troposphere and a deep, quiescent, lower layer representing the lower troposphere. The boundary between the layers represents a mid-tropospheric isentrope, across which mass can be exchanged in the presence of heating or cooling. This leads to the system

$$\frac{d\mathbf{v}}{dt} + g\nabla h + f\mathbf{k}\times\mathbf{v} = \mathbf{R} - \frac{\mathbf{v}}{\tau_{\rm drag}} \tag{1}$$

$$\frac{\partial h}{\partial t} + \nabla\cdot(\mathbf{v}h) = S - \frac{h}{\tau_{\rm rad}} \equiv Q \tag{2}$$

where $\mathbf{v}$ is horizontal velocity, h is layer thickness, and other notation is standard. The continuity equation (2) is forced by a mass source/sink S and damped by "radiative" relaxation over a timescale $\tau_{\rm rad}$. In the present context, mass sources and sinks represent regions of mid-tropospheric heating and cooling, respectively. The momentum equations (1) include drag with a timescale $\tau_{\rm drag}$, which could represent the

[1]Department of Planetary Sciences, Lunar and Planetary Laboratory, University of Arizona, Tucson, Arizona, USA.
[2]Department of Applied Physics and Applied Mathematics, Columbia University, New York, New York, USA.
[3]Lamont-Doherty Earth Observatory, Palisades, New York, USA.

0094-8276/10/2010GL044343

potentially important effects of momentum transport by cumulus convection [*Lin et al.*, 2008].

[6] The term **R** in equation (1) represents the effect on the upper layer of momentum advection from the lower layer, and takes the same form as that of *Shell and Held* [2004]:

$$\mathbf{R}(\lambda, \phi, t) = \begin{cases} -\frac{Q\mathbf{v}}{h}, & Q > 0; \\ 0, & Q < 0 \end{cases} \tag{3}$$

where λ and ϕ are longitude and latitude. Air moving out of the upper layer ($Q < 0$) does not locally affect the upper layer's specific angular momentum or wind speed, hence $\mathbf{R} = 0$ for that case. But air transported into the upper layer carries lower-layer momentum with it and thus alters the local specific angular momentum and zonal wind in the upper layer. For the simplest case where the lower layer winds are assumed to be zero, this process preserves the column-integrated $\mathbf{v}h$ of the upper layer, leading to the expression in (3) for $Q > 0$. Importantly, the expression for **R** follows directly from the momentum budget and contains no free parameters.

[7] As in the GCM studies of *Suarez and Duffy* [1992] and *Saravanan* [1993], we impose a tropical forcing S that is sinusoidal in longitude and gaussian in latitude:

$$S = \frac{h_0}{\tau_{\mathrm{rad}}} + S_0 \cos(m\lambda) \exp\left[-\left(\frac{\phi - \phi_0}{\Delta\phi}\right)^2\right] \tag{4}$$

where h_0 is a reference layer thickness, S_0 is the amplitude of the forcing, $m = 2$ is the zonal wavenumber, and $\Delta\phi = 20°$ is the latitudinal half-width of the heating. As in *Suarez and Duffy* [1992] and *Saravanan* [1993], we set $\phi_0 = 0°$ in most cases so that the imposed heating is symmetric about the equator. The GCM studies included, in addition to tropical heating variations, latitude-dependent forcing that generated meridional temperature gradients and baroclinic eddies in midlatitudes. We forgo any representation of these eddies here to investigate the mechanisms of superrotation (or lack thereof) in isolation.

[8] We solve the fully nonlinear, global, time-dependent forms of equations (1)–(3) in spherical geometry using the Spectral Transform Shallow Water Model (STSWM) of *Hack and Jakob* [1992]. The runs are integrated from rest using a T170 spectral truncation, corresponding to a resolution of 0.7° in longitude and latitude. A ∇^6 hyperviscosity maintains numerical stability. Up to moderate amplitudes the equilibrated solutions are steady. Unsteadiness sets in beyond a critical forcing amplitude, a phenomenon previously noted from shallow-water investigations with Gill-like forcing [*Hsu and Plumb*, 2000]. This phenomenon, while worthy of future study, does not affect the qualitative nature of our results. All solutions shown in this paper are equilibrated and steady.

3. Results

[9] Before solving the full set of equations (1)–(2), we note that, when **R** is dropped from equation (1), the system becomes identical to that of the standard Matsuno-Gill problem as examined by numerous authors [e.g., *Matsuno*, 1966; *Gill*, 1980; *Neelin*, 1988; *Bretherton and Sobel*, 2003]. It could be argued that neglecting **R** is unphysical, at least at large amplitude, because under these conditions the local momentum per area (integrated over both layers) is not conserved in the presence of mass exchange between the layers; such exchange introduces spurious sources or sinks of momentum. However, because the standard Matsuno-Gill formulation is a foundational model in tropical dynamics, we consider its solutions first.

[10] With $\mathbf{R} = 0$, we find that the solutions of equations (1)–(2) do not exhibit equatorial superrotation. Figure 1 (top) shows an example. The geopotential and wind fields show a strong resemblance to the Matsuno-Gill pattern (compare, for example, to *Matsuno* [1966, Figure 9]). Anticyclones and cyclones, essentially the steady Rossby-wave response, straddle the equator, while at the equator zonal flows diverge from mass source regions and converge toward mass sink regions; this is the Kelvin-wave component of the response. The zonal-mean zonal flow, $\overline{u}$, is zero at the equator and easterly in the subtropics, demonstrating that superrotation does not develop despite the existence of tropical forcing and wave-mean-flow interactions. Additional solutions over a wide range of parameters demonstrate that this is a robust result. Note that the absence of superrotation cannot result from the non-acceleration theorem: indeed, since the Matsuno-Gill model contains friction and thermal damping, the non-acceleration theorem does not apply at all.

[11] The orientations of the phase tilts in Figure 1a raise a puzzle as to why these solutions fail to exhibit equatorial superrotation. A pervasive feature of the solutions—also clear in the linear models of *Matsuno* [1966], *Gill* [1980] and subsequent studies—is that the velocity vectors near the equator tilt predominantly from northwest-to-southeast in the northern hemisphere and southwest-to-northeast in the southern hemisphere. These tilts indicate that $\overline{u'v'} < 0$ in the northern hemisphere and $\overline{u'v'} > 0$ in the southern hemisphere, suggesting an equatorward flux of westerly momentum. (Here, u' and v' are deviations of zonal and meridional wind from their zonal mean, and the overbar denotes zonal averaging.) This flux exhibits the correct sign to induce superrotation. The lack of superrotation illustrated in Figure 1 (top) is therefore surprising.

[12] To elucidate the absence of superrotation in the Matsuno-Gill problem, we analyze the zonal-momentum budget of the solutions to equations (1)–(2). Decomposing variables into their zonal means (denoted by overbars) and deviations therefrom (denoted with primes) and zonally averaging the zonal-momentum equation leads to [e.g., *Thuburn and Lagneau* 1999]

$$\frac{\partial \overline{u}}{\partial t} = \underbrace{\overline{v}^* \left[f - \frac{1}{a\cos\phi}\frac{\partial(\overline{u}\cos\phi)}{\partial\phi}\right]}_{I} \underbrace{- \frac{1}{\overline{h}a\cos^2\phi}\frac{\partial}{\partial\phi}\left[\overline{(hv)'u'}\cos^2\phi\right]}_{II} + \underbrace{\frac{1}{\overline{h}}\overline{u'Q'}}_{IIIa} + \underbrace{\overline{R_u}^*}_{IIIb} + \underbrace{\overline{X}^*}_{IV} - \frac{1}{\overline{h}}\frac{\partial\left(\overline{h'u'}\right)}{\partial t} \tag{5}$$

where a is the planetary radius and $\overline{A}^* \equiv \overline{hA}/\overline{h}$ denotes the thickness-weighted zonal average of any quantity A. In this equation, X refers to zonal friction, and for Rayleigh drag, $\overline{X}^* = -\overline{u}^*/\tau_{\mathrm{drag}}$. Equation (5) is the shallow-water version of the Transformed Eulerian Mean (TEM) momentum equation, analogous to that in the isentropic-coordinate form of the primitive equations [see *Andrews et al.*, 1987, section 3.9].

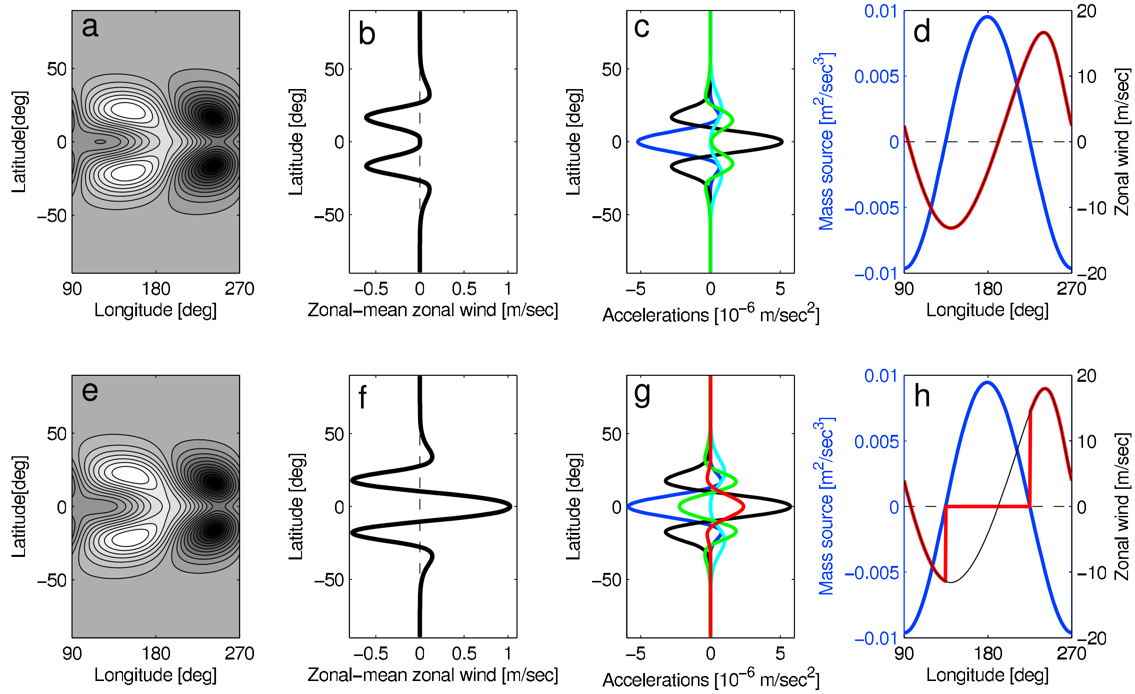

Figure 1. (top) A solution with $\mathbf{R}$ = 0 and (bottom) an otherwise identical solution with $\mathbf{R}$ given by equation (3). (a, e) Geopotential gh. (b, f) Zonal-mean zonal wind $\overline{u}$. (c, g) Accelerations of the zonal-mean zonal wind in the equilibrated state (see text). (d, h) Mass source Q at the equator (blue), zonal wind at the equator (*thin black*), and zonal wind at the equator that is advected into ($Q > 0$) or out of ($Q < 0$) the layer (red). Figures 1a, 1d, and 1e and 1h show only half the domain (longitudes 90° to 270°) for clarity. Both cases adopt $\tau_{\rm rad} = \tau_{\rm drag} = 5$ days, $\phi_0 = 0°$, $gh_0 = 4000{\rm m}^2\ {\rm sec}^{-2}$ (as given by *Gill* [1980]), and forcing amplitude $gS_0 = 0.0098{\rm m}^2\ {\rm sec}^{-3}$.

On the right-hand side, terms I, II, and III represent accelerations due to (i) momentum advection by the mean-meridional circulation, (ii) the convergence of the meridional flux of zonal eddy momentum, and (iii) correlations between the regions of eddy zonal flow and eddy mass source (essentially vertical eddy-momentum transport). The quantity R_u is the zonal component of $\mathbf{R}$ (equal to $-Qu/h$ when $Q > 0$ and 0 when $Q < 0$). Figure 1d depicts these terms for the equilibrated steady state; term IIIb is identically zero here.

[13] As expected, horizontal convergence of eddy momentum, term II, causes a strong westerly acceleration at the equator and easterly acceleration in the subtropics (Figure 1c, black curve). On the other hand, the acceleration associated with vertical eddy-momentum transport, term IIIa, is strong and easterly at the equator (dark blue). The cancellation between these two eddy terms explains the absence of superrotation. The remaining terms—the mean-meridional circulation (term I, light blue) and mass-weighted friction (term IV, green)—are small at the equator in the equilibrated state.

[14] The spatial velocity and mass source/sink patterns illuminate the physical origin of the easterly equatorial acceleration caused by the vertical eddy exchange. For the Matsuno-Gill problem, the longitudes of zero zonal wind at the equator lie east of the mass-source extrema (Figure 1d), a feature also clearly visible in the steady, linear calculations of *Matsuno* [1966, Figure 9], and *Gill* [1980, Figure 1]. Because of this shift, equatorial mass sources (sinks) occur predominantly in regions of easterly (westerly) eddy zonal flow. Hence, $\overline{u'Q'}$ is negative at the equator. When $\mathbf{R}$ = 0, therefore, both mass source and sink regions remove column-integrated westerly momentum from the layer, leading to a zonal-mean easterly acceleration that prevents the emergence of superrotation.

[15] Now envision the full system (1)–(2) including the vertical momentum advection term $\mathbf{R}$ as specified by (3). Equatorial mass-sink regions still locally decrease the column-integrated westerly momentum (since they transport air with net westerly momentum out of the layer; see Figure 1d). However, equatorial mass-source regions no longer alter the local, column-integrated relative momentum $\mathbf{v}h$ (since they bring up air with zero zonal wind, in contrast to the case when $\mathbf{R}$ = 0, in which case they spuriously decrease the column-integrated equatorial relative momentum). Thus, when zonally averaged, the vertical eddy terms still cause an easterly acceleration, but it is now weaker than for the case $\mathbf{R}$ = 0. As a result, the vertical eddy terms in (5) no longer fully cancel the latitudinal convergence of westerly eddy momentum. Superrotation should then occur. To test these arguments, we now solve equations (1)–(2), including $\mathbf{R}$ as given by (3).

[16] When the $\mathbf{R}$ term is included, superrotation emerges naturally. Figure 1 (bottom) illustrates the solution to equations (1)–(2) for the same parameter values as in Figure 1 (top). The geopotential fields of the two solutions are similar, and the qualitative zonal-mean zonal wind patterns coincide poleward of ~15° latitude. The primary difference is the emergence of equatorial superrotation—whose speed exceeds that of the zonal-mean zonal winds at any other latitude. Diagnostics (Figure 1g) demonstrate that, in the equilibrated (steady) state, the term $\overline{u'Q'}/\overline{h}$, (term IIIa, dark blue) still

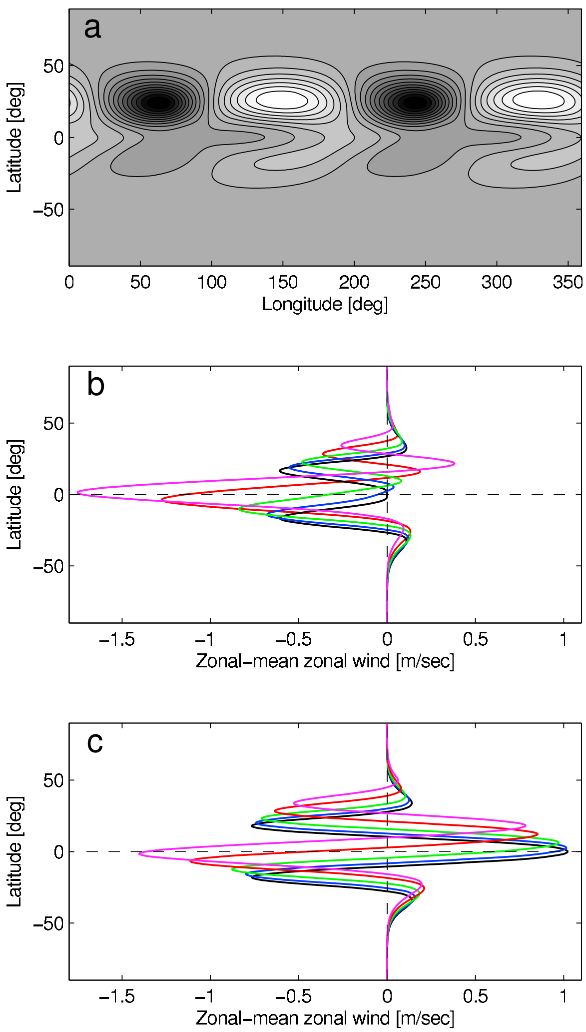

Figure 2. (a) Geopotential for a case identical to that in Figure 1 (top) except that the peak in heating is displaced 10° latitude north of the equator. (b) Zonal-mean zonal wind for a sequence of solutions with **R** = 0 (as in the standard Matsuno-Gill problem) and ϕ_0 = 0° (black), 2° (dark blue), 5° (green), 10° (red), and 15° (magenta). (c) Identical to Figure 2b but for a sequence of simulations with **R** given by equation (3).

largely cancels the horizontal eddy convergence at the equator (term II, black), but the term $\overline{R_u}^*$ (term IIIb, red) provides a westerly acceleration. As expected on intuitive grounds, the net vertical eddy terms—the sum of the dark blue and red curves—still cause an easterly equatorial acceleration, but it no longer fully counteracts the westerly acceleration induced by horizontal eddy momentum convergence. Momentum balance only occurs when superrotation emerges and becomes sufficiently strong for the easterly equatorial acceleration due to friction to balance the mismatch in the eddy terms.

[17] In our model, the role of momentum exchange between the active and abyssal layer (represented by **R**) differs significantly from that explored by *Shell and Held* [2004], who solved an axisymmetric, but otherwise similar, 1-1/2 layer shallow-water model. Because their model contains no equatorial eddies, the velocity entering their expression for **R** is the zonal-mean value, implying that in their case **R** causes an easterly drag that resists the superrotation. For the Matsuno-Gill problem explored here, however, equatorial mass-source regions that contribute to **R** flow predominantly easterly even in the presence of superrotation. Thus, **R** contributes a westerly acceleration that *enables* superrotation. An implication of this mechanism is that the zonal-mean zonal wind speeds in the superrotating jet cannot exceed the eddy zonal velocity.

[18] To investigate whether superrotation emerges in cases when symmetry about the equator plays no role, we performed a series of integrations with the heating maximum displaced up to 15° off the equator. Cases where ϕ_0 is tiny but nonzero—to break the symmetry—differ negligibly from otherwise equivalent cases where ϕ_0 = 0°. Solutions with finite ϕ_0 retain the qualitative features of the original solutions but become asymmetric about the equator (see Figure 2a for an example). When **R** = 0, finite displacements lead to *easterly* zonal-mean zonal flow at the equator (Figure 2b) as the region of net easterly eddy acceleration (originally in the subtropics) moves onto the equator. These results demonstrate that the lack of superrotation when **R** = 0 is a general result of the Matsuno-Gill model and not a quirk of symmetry. When **R** is included (Figure 2c), equatorial superrotation still occurs, as long as ϕ_0 is not too large.

4. Discussion

[19] We argue that our 1-1/2 layer model with Matsuno-Gill-type forcing captures—in its essence—the mechanism responsible for generating equatorial superrotation in idealized GCMs forced by steady tropical heating [*Suarez and Duffy*, 1992; *Saravanan*, 1993; *Kraucunas and Hartmann*, 2005; *Norton*, 2006]. The near cancelation at the equator between the horizontal and vertical eddy momentum convergences (terms II and III in equation (5)), with the horizontal convergence slightly favored, also occurs in the idealized GCMs [e.g., see *Norton*, 2006, Figures 7b and 7d].

[20] We find that superrotation occurs at all forcing amplitudes, even arbitrarily small amplitudes where the solutions behave linearly. This contrasts with the case examined by *Suarez and Duffy* [1992] and *Saravanan* [1993], where superrotation only developed for forcing amplitudes exceeding a threshold value. In their case, the tropical wave forcing only triggers superrotation when it attains sufficiently great amplitudes to overcome the easterly torques provided by the Hadley circulation and midlatitude eddies propagating into the tropics. Our model, which lacks a Hadley circulation and midlatitude eddy forcing, allows us to conclude that the mechanism for generating superrotation has no inherent threshold.

[21] To emphasize the connection between our solutions and the steady, linear calculations of *Matsuno* [1966] and *Gill* [1980], we intentionally chose for illustration a low-amplitude case with a thin layer and equal radiative and drag time constants (Figure 1). This leads to a solution with a modest zonal-mean zonal wind speed. However, solutions with Earth-like speeds of 30 msec^{-1} or more are easily achievable with stronger forcing amplitudes and drag time constants that substantially exceed the radiative time constants.

[22] The arguments presented here suggest that equatorial superrotation could arise in past or future climates—or on other planets—if the tropical wave forcing is strong or the factors resisting it (Hadley circulation and midlatitude eddy

forcing) are weak. Jupiter and Saturn, for example, exhibit equatorial superrotation; if atmospheric convection near the equator becomes organized on the large-scale—developing organized longitudinal contrasts in latent heating, for example—superrotation might emerge through the mechanism discussed here. Moreover, "hot Jupiters"—gas giants orbiting other stars at very close orbital separations—have enormous day-night radiative heating contrasts and also develop equatorial superrotation in three-dimensional circulation models [e.g., *Showman et al.*, 2009], probably by the same mechanism as discussed here.

[23] **Acknowledgments.** This work was supported by a NASA grant to APS and an NSF grant to LMP.

References

Andrews, D. G., J. R. Holton, and C. B. Leovy (1987), *Middle Atmosphere Dynamics*, Academic, New York.

Biello, J. A., A. J. Majda, and M. W. Moncrieff (2007), Meridional momentum flux and superrotation in the multiscale IPESD MJO model, *J. Atmos. Sci.*, *64*, 1636–1651.

Bretherton, C. S., and A. H. Sobel (2003), The Gill model and the weak temperature gradient approximation, *J. Atmos. Sci.*, *60*, 451–460.

Caballero, R., and M. Huber (2010), Spontaneous transition to superrotation in warm climates simulated by CAM3, *Geophys. Res. Lett.*, *37*, L11701, doi:10.1029/2010GL043468.

Gill, A. E. (1980), Some simple solutions for heat-induced tropical circulation, *Q. J. R. Meteorol. Soc.*, *106*, 447–462.

Hack, J. J., and R. Jakob (1992), Description of a global shallow water model based on the spectral transform method, *NCAR Tech. Rep. NCAR/TN-343+STR*, Natl. Cent. for Atmos. Res., Boulder, Colo.

Held, I. M. (1999), Equatorial superrotation in Earth-like atmospheric models, Bernhard Haurwitz Memorial Lecture, Am. Meteorol. Soc., Boston, Mass. (Available at www.gfdl.noaa.gov/isaac-held-homepage)

Hsu, C. J., and R. A. Plumb (2000), Nonaxisymmetric thermally driven circulations and upper-tropospheric monsoon dynamics, *J. Atmos. Sci.*, *57*, 1255–1276.

Kraucunas, I., and D. L. Hartmann (2005), Equatorial superrotation and the factors controlling the zonal-mean zonal winds in the tropical upper troposphere, *J. Atmos. Sci.*, *62*, 371–389.

Lee, S. (1999), Why are the climatological zonal winds easterly in the equatorial upper troposphere?, *J. Atmos. Sci.*, *56*, 1353–1363.

Lin, J., B. E. Mapes, and W. Han (2008), What are the sources of mechanical damping in Matsuno Gill-type models?, *J. Clim.*, *21*, 165–179.

Matsuno, T. (1966), Quasi-geostrophic motions in the equatorial area, *J. Meteorol. Soc. Jpn.*, *44*, 25–43.

Neelin, J. D. (1988), A simple model for surface stress and low-level flow in the tropical atmosphere driven by prescribed heating, *Q. J. R. Meteorol. Soc.*, *114*, 747–770.

Norton, W. A. (2006), Tropical wave driving of the annual cycle in tropical tropopause temperatures. Part II: Model results, *J. Atmos. Sci.*, *63*, 1420–1431.

Saravanan, R. (1993), Equatorial superrotation and maintenance of the general circulation in two-level models, *J. Atmos. Sci.*, *50*, 1211–1227.

Shell, K. M., and I. M. Held (2004), Abrupt transition to strong superrotation in an axisymmetric model of the upper troposphere, *J. Atmos. Sci.*, *61*, 2928–2935.

Showman, A. P., J. J. Fortney, Y. Lian, M. S. Marley, R. S. Freedman, H. A. Knutson, and D. Charbonneau (2009), Atmospheric circulation of hot Jupiters: Coupled radiative-dynamical general circulation model simulations of HD 189733b and HD 209458b, *Astrophys. J.*, *699*, 564–584.

Suarez, M. J., and D. G. Duffy (1992), Terrestrial superrotation: A bifurcation of the general circulation, *J. Atmos. Sci.*, *49*, 1541–1556.

Thuburn, J., and V. Lagneau (1999), Eulerian mean, contour integral, and finite-amplitude wave activity diagnostics applied to a single-layer model of the winter stratosphere, *J. Atmos. Sci.*, *56*, 689–710.

Tziperman, E., and B. Farrell (2009), Pliocene equatorial temperature: Lessons from atmospheric superrotation, *Paleoceanography*, *24*, PA1101, doi:10.1029/2008PA001652.

L. M. Polvani, Department of Applied Physics and Applied Mathematics, Columbia University, 500 West 120th St., New York, NY 10027, USA.

A. P. Showman, Department of Planetary Sciences, Lunar and Planetary Laboratory, University of Arizona, 1629 E. University Blvd., Tucson, AZ 85721, USA. (showman@lpl.arizona.edu)